KJO
pISSN: 1011-8942 eISSN: 2092-9382

Korean J Ophthalmol 2019;33(1):70-81
https://doi.org/10.3341/kjo.2018.0085

Original Article

Analysis of Positional Relationships of Various Centers in Cataract Surgery

Woo Keun Song, Jin Ah Lee, Jae Yong Kim, Myoung Joon Kim, Hungwon Tchah

Department of Ophthalmology, Asan Medical Center, University of Ulsan College of Medicine, Seoul, Korea

Purpose: To analyze the positional relationships of various centers in patients undergoing femtosecond laser-assisted cataract surgery (FLACS).

Methods: The locations of the pupil center (PC), limbal center (LC) and lens center were analyzed in each patient using optical coherence tomography during FLACS in 35 eyes of 35 patients. Using the preoperative corneal aberrometry device, angle kappa and the location of the visual axis (VA) were calculated. After acquiring the relative horizontal and vertical coordinates of each center, the distance and location among each center were compared. The relative location and distance of each center were statistically evaluated.

Results: The distance from the PC to the lens center was 0.147 ± 0.103 mm, that from the LC to the lens center was 0.205 ± 0.104 mm, and that from the VA to the lens center was 0.296 ± 0.198 mm. The distance from the PC to the VA was 0.283 ± 0.161 mm, that from the LC to the VA was 0.362 ± 0.153 mm, and that from the lens center to the VA was 0.296 ± 0.198 mm. Among the various centers, the PC was the closest to the lens center, whereas the LC and VA were the farthest. Based on the location of the lens center, the PC, LC, and VA exhibited differences in the X and Y coordinate positions (vertical $p = 0.004$, horizontal $p < 0.001$). Among them, the LC was significantly inferior and temporal compared to the PC (vertical $p = 0.026$, horizontal $p = 0.023$). Based on the location of the VA, the respective locations of the PC, LC and lens center in two dimensions did not significantly differ (vertical $p = 0.310$, horizontal $p = 0.926$).

Conclusions: This study demonstrated the positional and locational relationships between the centers regarding FLACS. The locations of the PC, LC, and VA were different from the lens center with the PC being the closest. Surgeons should be aware of these positional relationships, especially in FLACS.

Key Words: Angle kappa, Lens center, Limbal center, Pupil center, Visual axis

Continuous curvilinear capsulorhexis (CCC), which was first introduced by Gimbel and Neuhann, is a conventional technique in cataract surgery [1,2]. CCC is one of the most important stages among various cataract surgery procedures due to its influence on the position of intraocular lens (IOL) after IOL implantation [3]. IOL malposition and poor vision can be caused by complications resulting from abnormal CCC procedures. Therefore, adequate and appropriate size, location and shape of CCC are consistently emphasized in cataract surgery [4-6]. However, the size, location, and shape of manual CCC may vary according to cataract type and surgeon experience.

There are various anatomical centers in cataract surgery. Pupil center (PC) and limbal center (LC), the centers of the pupil and limbus, respectively, are easily identified in the surgical field using a microscope and are commonly

Received: July 25, 2018 *Accepted*: October 1, 2018

Corresponding Author: Hungwon Tchah, MD, PhD. Department of Ophthalmology, Asan Medical Center, University of Ulsan College of Medicine, 88 Olympic-ro 43-gil, Songpa-gu, Seoul 05505, Korea. Tel: 82-2-3010-3674, Fax: 82-2-470-6440, E-mail: hwtchah@amc.seoul.kr

used for conventional cataract surgery when performing the CCC procedure. The lens center, which is also called the scanned capsule center, can be analyzed using software built into the device used in femtosecond laser-assisted cataract surgery. The location of the lens center can be calculated and interpreted based on extrapolation of the anterior and posterior capsule lines of the crystalline lens using the Catalys femtosecond laser software (Fig. 1A-1C).

In addition, with recent advancements in the precision of refractive surgery and multifocal IOL (MFIOL) implantation in cataract surgery, angle kappa remains an important consideration in improving visual outcomes [7]. Angle kappa is of considerable importance in refractive surgery outcomes and may play a role in MFIOL decentration, which can increase glare and halo [8-10]. Numerous studies suggest that moving the center of ablation away from the PC and towards the visual axis (VA) may improve the quality and durability of visual outcomes, especially in hyperopic laser-assisted *in situ* keratomileusis (LASIK) patients [11,12]. Therefore, angle kappa and the location of the VA must be considered from the perspective of postoperative visual outcomes.

Most surgeons perform CCC in cataract surgery based on the PC. However, considering the anatomical structure of the crystalline lens capsular bag and IOL centration, the positional relationship of various centers in cataract surgery must be taken into account. Therefore, we analyzed the positional relationships of various centers using devices available for preoperative evaluation of cataract surgery and assessed their clinical significance.

Materials and Methods

Subjects

Thirty-five eyes of 35 patients who had undergone uneventful cataract surgery with femtosecond laser-assistance by a single surgeon (HT) were reviewed in this study. The medical records of all subjects who underwent cataract surgery from April 2016 to January 2017 in clinic of the Asan Medical Center in Seoul, Korea were retrospectively reviewed. Subjects with intraoperative or postoperative complications or a history of ocular trauma history or intraocular surgical procedures were excluded from this study. Individuals with past or present ocular disease other than cataracts were also excluded from this study. The study protocol was approved by the institutional review board of the Asan Medical Center (2017-0526), and the study design followed the principles of the Declaration of Helsinki.

Preoperative and postoperative ophthalmologic examination and surgical procedures

Initial testing comprised comprehensive ophthalmologic examination, including a review of patient medical history, measurement of best-corrected visual acuity (BCVA), performance of slit-lamp biomicroscopy, and funduscopy. Preoperative and postoperative refraction and keratometry were measured via manifest refraction and automated keratometry and refraction. Grades of nuclear sclerosis and cortical sclerosis were evaluated with slit-lamp biomicroscopy using the Lens Opacities Classification System III by a single examiner (HT) with dilation of the pupil of the affected eye. Axial length was measured using IOLMaster Optical Biometry (Carl Zeiss, Jena, Germany). The affected eyes of all the participants were imaged with AS-OCT (Visante ver. 2.0; Carl Zeiss Meditec, Jena, Germany) operating in the enhanced anterior segment single mode (scan length, 16 mm; 256 A-scans). Specular microscopy (EM-3000; Tomey, Nagoya, Japan), corneal topography, and aberrometry including the OPD Scan III (Nidek, Gamagori, Japan) were also performed preoperatively.

Femtosecond laser-assisted cataract surgery was performed using a Catalys precision laser system (Abbott Medical Optics, Santa Ana, CA, USA). All of the procedures were performed by one surgeon (HT). The sequence of laser treatment steps involved initial capsulotomy (4.8 to 4.9 mm diameter), lens fragmentation, and then intrastromal arcuate incisions at the intended meridian. The programmed intrastromal arcuate incision parameters were 20% uncut anterior, 20% uncut posterior, and 90° side cut angle at an 8.0-mm optical zone. In the lens fragmentation step, the fragmentation pattern and number were decided according to the grade of nuclear and cortical sclerosis from 700 μm above the posterior capsule to 500 μm below the anterior capsule.

Ideal CCC size is generally 5.0 to 5.5 mm [13]. However, in this study, a relatively small CCC was performed during femtosecond laser-assisted cataract surgery. The main reason for the small CCC size was to maintain the effective lens position to ensure the stability of CCC. Small-sized CCC deepens the anterior chamber so that the surgeon can

easily control effective lens position [14]. In addition, a 0.5-mm minimum margin from the pupil is usually recommended during femtosecond laser-assisted cataract surgery capsulotomy. There were several cases of poor pupil dilation; thus, CCC size had to be smaller than usual.

Arcuate incisions were performed in eyes with corneal astigmatism over 1.5 diopters. To determine the arc length of the intrastromal incision, an Intrastromal AK nomogram calculator proposed by Julian Stevens (http://femtoemulsification.com/) was modified to take into account posterior corneal astigmatism.

After the confirmation of incisions and capsulotomy flap creation using the femtosecond laser, hydrodissection and phacoemulsification with the OZil torsional system (Infiniti; Alcon, Fort Worth, TX, USA) were performed. A foldable posterior chamber IOL was implanted into the capsular bag. The IOLs used in this study were one-piece acrylic versions (TECNIS ZCB00, Abbott Medical Optics; Hoya iSert 250, Hoya Surgical Optics, Tokyo, Japan). No intraoperative complications occurred. The power of the implanted IOL was calculated for each patient using preoperative biometric data and the IOL power formula.

Analysis of the relative location of centers

As mentioned above, using the femtosecond laser Catalys system device and software, the locations of the PC, LC, and lens center can automatically be identified through the acquisition of transformed images and video files (Fig. 1). The location of the lens center is calculated via extrapolation of the anterior and posterior capsule lines of the crystalline lens through the built-in Catalys system device (Fig. 1, 2). The locational parameters of the centers were determined using ImageJ software ver. 1.46 (National Institutes of Health, Bethesda, MD, USA), and the relative location of and distance between each center were evaluated. The real distance per pixel (X-axis and Y-axis) was calculated, using images with the same resolution by dividing the real distance of the CCC diameter by the number of pixels of the CCC diameters (Fig. 3A-3C). CCC diameter, which varied from 4.8 to 4.9 mm, was shown in the femtosecond laser software. On the horizontal plane, the nasal side was defined as a negative value, while the temporal side was defined as a positive value. Location on the vertical plane was described using the same method, with the superior side defined as positive and the inferior side as negative.

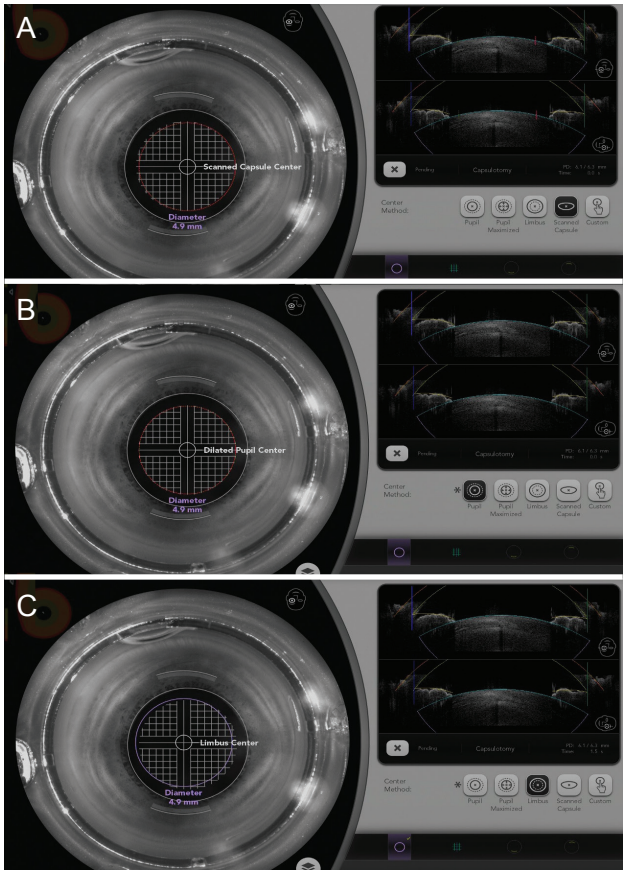

Fig. 1. Location of each center. (A) Lens center, (B) pupil center, and (C) limbal center.

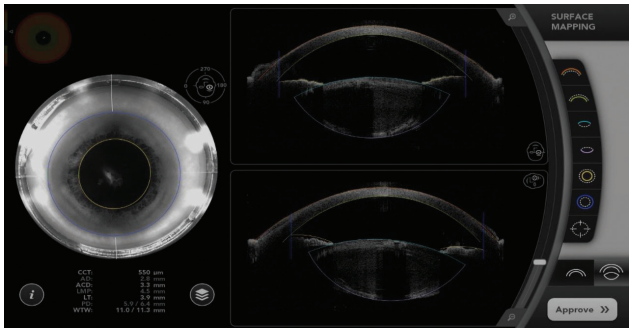

Fig. 2. Extrapolation of anterior and posterior capsular lines in the crystalline lens.

Using the angle kappa concept, the location of the VA can be calculated using corneal topography and aberrometry devices. In this study, the location of the VA was calculated using an OPD Scan III device. OPD Scan III images were acquired with the eyes in a preoperative pharmacologically dilated state (Fig. 4). Since we could determine

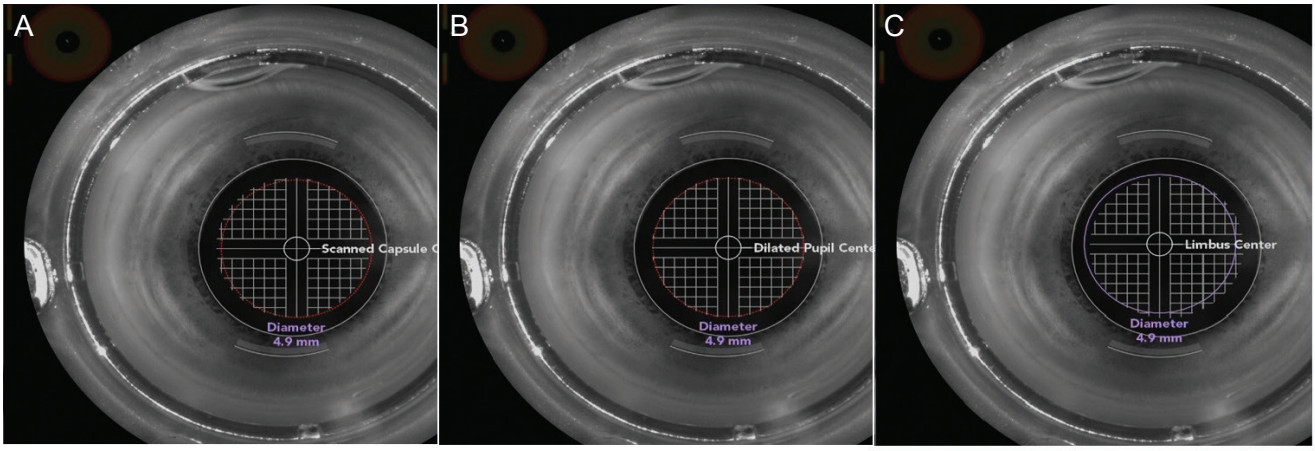

Fig. 3. Calculation of the distances between the pupil, limbal and lens centers. Pixels for each center were acquired using ImageJ software. (A) Lens center, (B) pupil center, and (C) limbal center.

the distance and relative angle between the PC and VA using the acquired images, the horizontal and vertical locations of the VA can be calculated based on the PC. Having established the relative horizontal and vertical coordinates of each center, the distances between the centers were calculated using the Pythagorean formula. The parameters and values in each image were evaluated by an independent examiner (WKS) who was blinded to all other test results and to the clinical information of the participants.

$$\text{Real distance per X-axis pixel} = \frac{\text{CCC diameter}}{\text{X-axis pixel in CCC diameter}}$$

$$\text{X-axis distance between centers}^2 + \text{Y-axis distance between centers}^2 = \text{real distance between centers}^2$$

Statistical analysis

All statistical analyses were performed using commercial software (IBM SPSS Statistics ver. 24.0; IBM Corp., Armonk, NY, USA). The differences between the centers were evaluated statistically using one-way ANOVA. Relative horizontal and vertical locations were analyzed using Pearson's chi-square test. The association between angle kappa and the distance between centers was evaluated via linear regression analysis, and the difference between the distances according to angle kappa was analyzed using independent sample *t*-tests. A *p*-value of <0.05 was considered statistically significant.

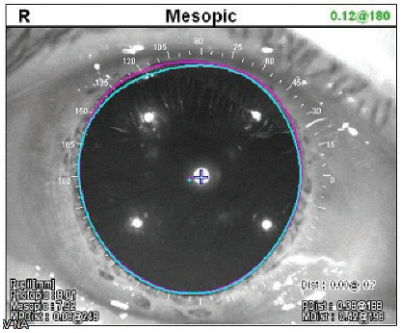

Fig. 4. Location of the pupil center and visual axis on OPD scan III in a pharmacologically dilated state. The blue and pink centers are the photopic and mesopic pupil centers, respectively, and the large central plus sign represents the visual axis. PDist and MDist denote the distance between the pupil center and the visual axis in the photopic and mesopic states, respectively.

Results

Baseline and femtosecond laser-related characteristics

Thirty-five eyes of 35 cataract patients who underwent uneventful cataract surgery were included in this study. Mean age was 61.34 ± 17.64 years and 28 of the 35 patients were male. The mean nuclear sclerosis grade was 3.98 ± 1.58, and the mean cortical sclerosis grade was 3.50 ± 1.00 according to Lens Opacities Classification System III classification. The mean BCVA (logarithm of the minimum angle of resolution) before cataract surgery was 0.31 ± 0.19, and postoperative 1-month mean BCVA was 0.05 ± 0.07, showing significant visual acuity improvement ($p < 0.001$).

Table 1. Preoperative demographic and clinical characteristics

	Mean ± SD	Range
Age (yr)	61.34 ± 17.64	46 to 91
Sex (male : female)	13 : 22	
Eye (right : left)	16 : 19	
Preoperative BCVA (logMAR)	0.31 ± 0.19	0.1 to 1.0
Preoperative astigmatism (D)	1.10 ± 0.75	0.25 to 3.5
Preoperative refraction (SE)	-0.68 ± 2.25	-6.25 to +2.25
Axial length (mm)	23.44 ± 1.04	21.95 to 26.35
Endothelial cell count	2,635.32 ± 251.27	2,299 to 3,096
Nucleus grade	3.98 ± 1.58	2 to 6
Cortex grade	3.50 ± 1.00	2 to 5
Dilated pupil size (mm)	6.96 ± 0.67	6.1 to 8.5
Anterior chamber depth (mm)	3.56 ± 0.44	2.5 to 4.5
Lens thickness (mm)	4.44 ± 0.56	3.4 to 5.6
Angle kappa (°)	5.14 ± 1.63	3.01 to 8.92

Values are presented as mean ± standard deviation.
SD = standard deviation; BCVA = best-corrected visual acuity; logMAR = logarithm of the minimum angle of resolution; D = diopters; SE = spherical equivalent.

Table 2. Postoperative clinical characteristics

	Mean ± SD	Range
Postoperative BCVA (logMAR)	0.05 ± 0.07	0.0 to 0.2
Postoperative refraction (SE)	-0.39 ± 0.75	-3.75 to +1.00
Postoperative astigmatism (D)	0.70 ± 0.27	0.25 to 1.25

SD = standard deviation; BCVA = best-corrected visual acuity; logMAR = logarithm of the minimum angle of resolution; SE = spherical equivalent; D = diopters.

The mean preoperative astigmatism was 1.10 ± 0.75 D, while the mean 1-month postoperative astigmatism was 0.70 ± 0.27 diopters, indicating a significant decrease in astigmatism (p = 0.013). The mean angle kappa value was 5.14 ± 1.63°. Tables 1 and 2 summarize pre- and postoperative clinical data. The mean CCC diameter measured by femtosecond laser software was 4.83 ± 0.13 mm. A paired arcuate incision was performed in 71.4% of all eyes.

Distance of centers from the lens center

First, we analyzed the location of the centers by distance based on the location of the lens center and VA. The distance from the PC to the lens center was 0.147 ± 0.103 mm, the distance from the LC to the lens center was 0.205 ± 0.104 mm, and the distance from the VA coordinates to the lens center was 0.296 ± 0.198 mm. The difference between the distance from the PC to the lens center and from the LC to the lens center was 0.058 ± 0.158 mm (p = 0.036), the difference between the distance from the LC to the lens center and from the VA coordinates to the lens center was 0.091 ± 0.227 mm (p = 0.024), and the difference between the distance from the VA coordinates to the lens center and the distance from the PC to the lens center was 0.149 ± 0.34 mm (p < 0.001). The PC was closest to the lens center, whereas the LC and VA were farther away on multiple comparisons analysis (Table 3 and Fig. 5A, 5B).

Distance of centers from the VA

Using the same method, we evaluated the location of the centers based on the VA. The distance from the PC to the VA coordinates was 0.283 ± 0.161 mm, the distance from the LC to the VA coordinates was 0.362 ± 0.153 mm, and the distance from the lens center to the VA coordinates was 0.296 ± 0.198 mm. There was no significant difference among these three distances (p = 0.125). According to the mean value, the PC tends to be located closest to the lens center compared to the other centers, but this difference was not statistically significant (Table 4 and Fig. 5).

Table 3. Distance between the lens center and other centers

	PC–lens center	LC–lens center	VA–lens center	*p*-value*
Mean distance ± SD	0.147 ± 0.103	0.205 ± 0.104	0.296 ± 0.198	<0.001
Range	0.025 to 0.417	0.081 to 0.493	0.038 to 0.864	

PC = pupil center; LC = limbal center; VA = visual axis; SD = standard deviation.
*One-way ANOVA, Bonferroni post-hoc test.

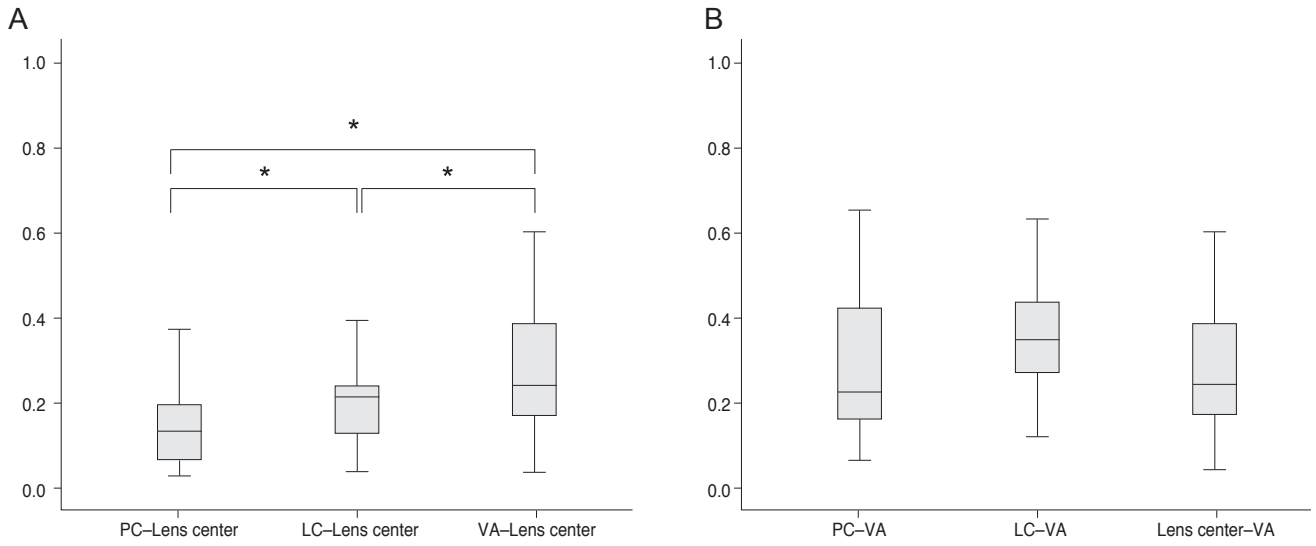

Fig. 5. Distance between centers. (A) Distance between centers and the lens center and (B) distance between centers and the visual axis (VA). PC = pupil center; LC = limbal center. *Statistically significant.

Table 4. Distance between the VA and various centers

	PC–VA	LC–VA	Lens center–VA	*p*-value*
Mean distance ± SD	0.283 ± 0.161	0.362 ± 0.153	0.296 ± 0.198	0.125
Range	0.060 to 0.650	0.118 to 0.923	0.038 to 0.864	

VA = visual axis; PC = pupil center; LC = limbal center; SD = standard deviation.
*One-way ANOVA, Bonferroni post-hoc test.

Table 5. Location of the pupil, limbal center and visual axis relative to the lens center

	Superior	Inferior	Temporal	Nasal
Pupil center	13	19	14	16
Limbal center	5	27	26	9
Visual axis	19	16	5	30
p-value*	0.004		<0.001	

*Chi-square test.

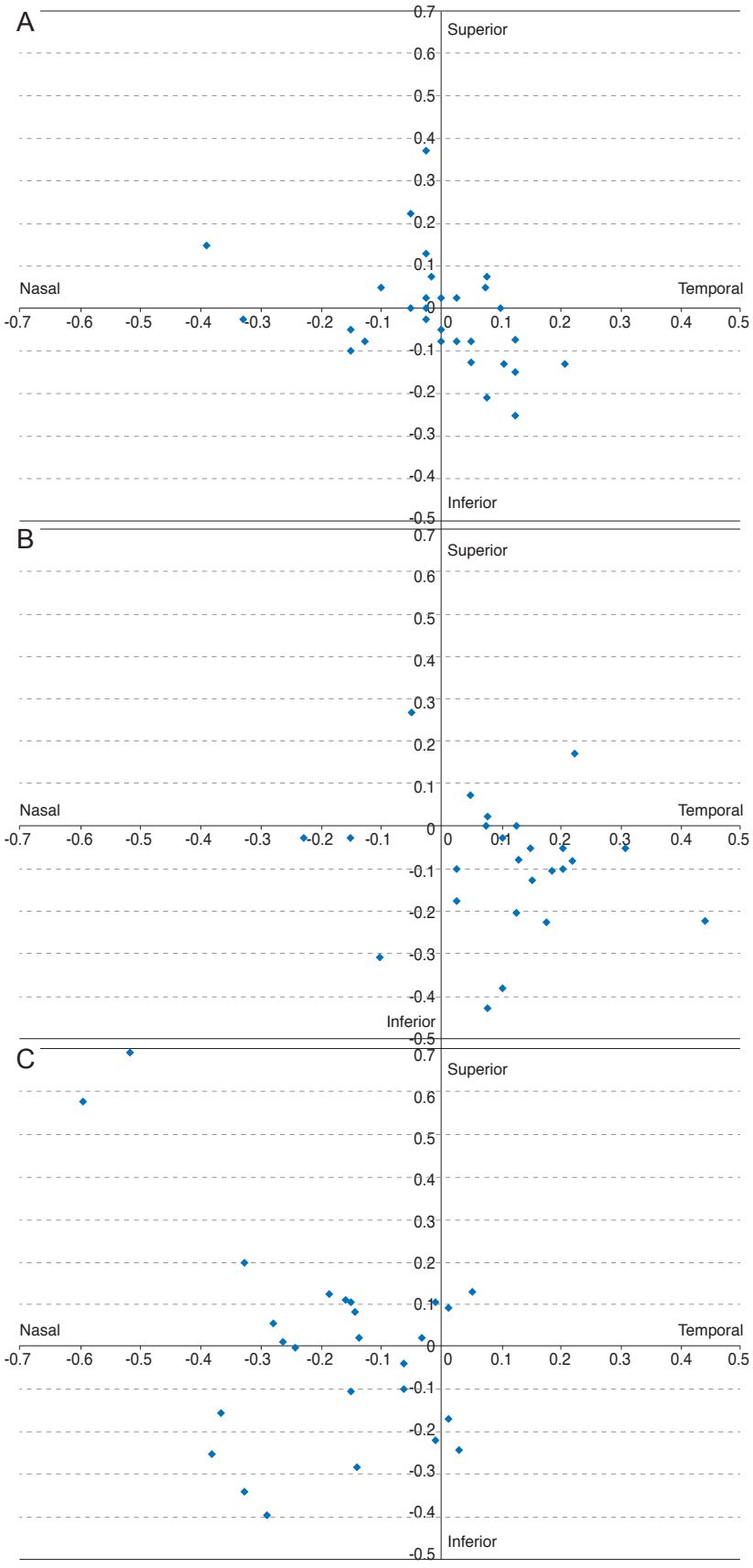

Fig. 6. Location of the pupil, limbal center and visual axis relative to the lens center. (A) Relative pupil center location, (B) relative limbal center location, and (C) relative visual axis location.

Location between the centers based on the lens center and the VA

The location of the pupil, limbal, lens centers and VA are presented as a two-dimensional scatterplot with the position of the lens center or VA as the origin. Based on the location of the lens center, the PC, LC and the coordinates of the VA showed had significantly different X and Y coordinate positions (chi-square test, vertical $p = 0.004$, horizontal $p < 0.001$) (Table 5 and Fig. 6A-6C). Based on the location of the lens center, the LC was significantly inferior and temporal in location compared to the PC (chi-square test, vertical $p = 0.026$, horizontal $p = 0.023$). Coordinate values of the PC, LC and VAequal to the vertical and horizontal coordinates of the lens center were excluded from data analysis.

Based on the location of the VA, the respective locations of the pupil, limbal, and lens centers in two dimensions did not vary significantly (chi-square test, vertical $p = 0.310$, horizontal $p = 0.926$) (Table 6 and Fig. 7A-7C).

Angle kappa and distance between centers

Among preoperative biometric factors, angle kappa has important clinical significance because of its impact on the postoperative visual quality. Therefore, we investigated the associations between angle kappa and distance between the centers using univariate regression analysis. Angle kappa affects the distance between the PC and VA ($p = 0.017$) (Table 7). Larger angle kappa is associated

Table 7. Univariate analysis of associations between angle kappa and the distance between centers

	β (95% CI)	*p*-value*
PC–lens center	-0.142 (-7.183 to 3.049)	0.417
LC–lens center	-0.048 (-5.835 to 4.428)	0.782
VA–lens center	0.195 (-1.172 to 4.173)	0.262
PC–VA	0.401 (0.723 to 6.872)	0.017
LC–VA	0.135 (-2.163 to 4.853)	0.441

β = standardized beta coefficient; CI = confidence interval; PC = pupil center; LC = limbal center; VA = visual axis.

Table 6. Location of the pupil, limbal and lens centers relative to the visual axis

	Superior	Inferior	Temporal	Nasal
Pupil center	15	20	32	3
Limbal center	10	25	31	4
Lens center	16	19	30	5
p-value*	0.310	0.926		

*Chi-square test.

Table 8. Difference in the distance between centers according to angle kappa

	Angle kappa	Number	Mean ± SD	Difference (95% CI)	*p*-value*
PC–lens center	<5°	15	0.257 ± 0.232	0.030 (-0.043 to 0.103)	0.406
	>5°	20	0.326 ± 0.169		
LC–lens center	<5°	15	0.245 ± 0.081	0.069 (-0.001 to 0.139)	0.053
	>5°	20	0.176 ± 0.113		
VA–lens center	<5°	15	0.257 ± 0.232	-0.069 (-0.207 to 0.068)	0.314
	>5°	20	0.326 ± 0.169		
PC–VA	<5°	15	0.243 ± 0.158	-0.070 (-0.181 to 0.041)	0.209
	>5°	20	0.313 ± 0.161		
LC–VA	<5°	15	0.342 ± 0.129	-0.035 (-0.142 to 0.072)	0.505
	>5°	20	0.377 ± 0.170		

Values are presented as mean ± standard deviation.
SD = standard deviation; CI = confidence interval; PC = pupil center; LC = limbal center; VA = visual axis.
*Independent sample *t*-test.

77

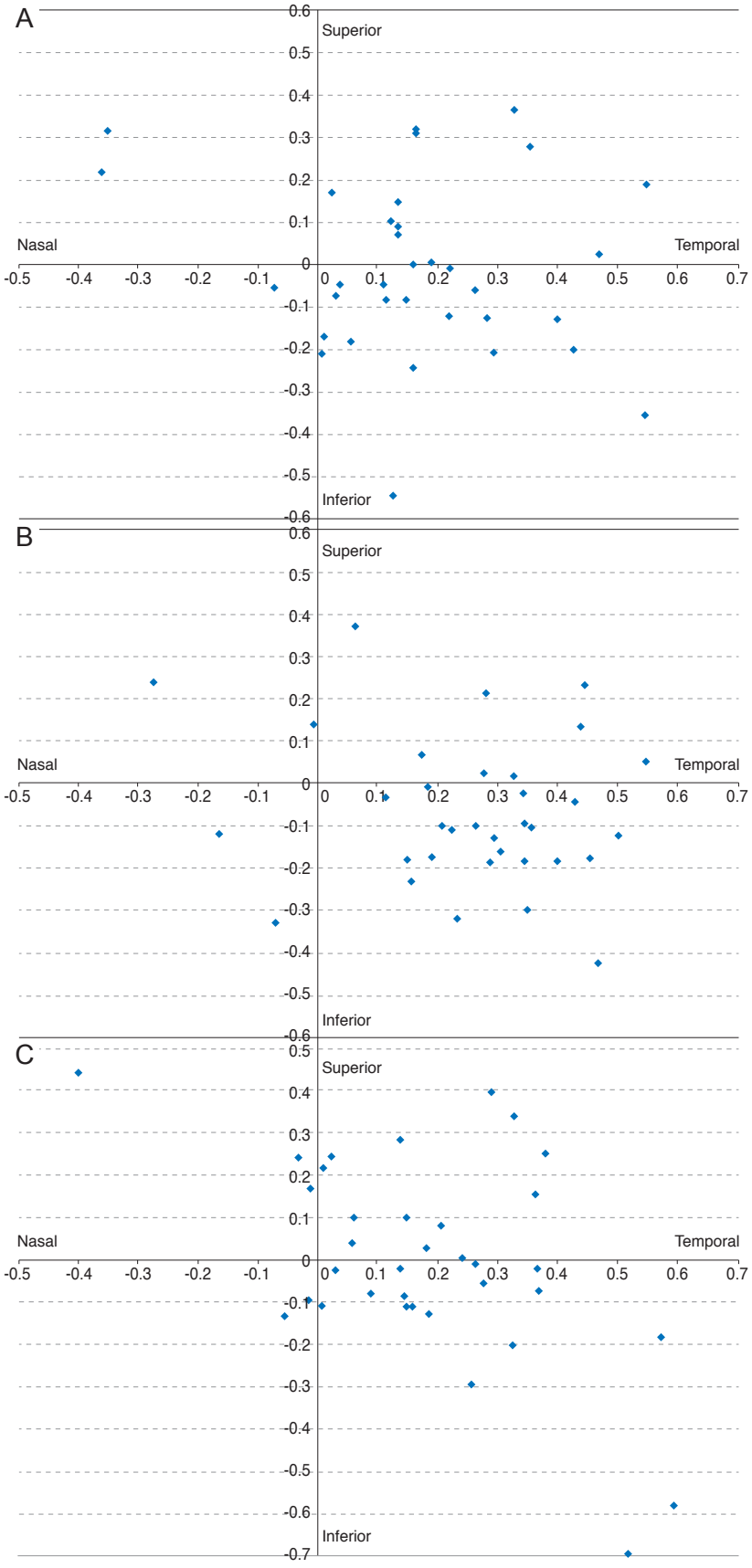

Fig. 7. Location of the pupil, limbal and lens centers relative to the visual axis. (A) Relative pupil center location, (B) relative limbal center location, and (C) relative lens center location.

78

with greater PC-VA distance (β = 0.401). Considering the definition of angle kappa, this result can be easily understood. However, other distances between centers had no significant linear correlations with angle kappa (Table 7). To clarify the relationship between angle kappa and distances between centers, we set the angle kappa value based on a cutoff criterion of 5°. Distances between centers were not significantly correlated with angle kappa (Table 8).

Discussion

This study identified various locational relationships between centers in not only the PC and LC, which are easily recognizable and used conventionally, but also the lens center and VA, which have anatomical and functional implications for visual outcomes. In terms of clinical significance, the locations and positional relationships of various centers are applicable in the CCC of cataract surgery with MFIOL implantation.

Abnormal size, shape and location of the CCC can result in abnormal IOL position, such as tilting or dislocation [15]. These outcomes are related to postoperative refractive and high-order aberration changes, which are major risk factors for poorer visual outcomes after cataract surgery. Therefore, numerous studies emphasize adequate CCC, especially in femtosecond laser-assisted cataract surgery [16-18]. Femtosecond laser-assisted cataract surgery is superior to manual cataract surgery due to significantly reduced IOL horizontal tilting and higher circularity, as well as decreased high-order aberration and mean refractive error, all of which are related to more precise anterior capsulorhexis in femtosecond laser-assisted cataract surgery [18-21].

Anatomically, if there are no intraoperative complications during cataract surgery, IOL optic and spring-like haptic structures are implanted into the capsular bag during the IOL insertion stage. The position of the IOL center will be similar to the center of the crystalline lens. Therefore, to counteract the contraction force that is related to IOL tilting and decentration that can occur after cataract surgery, CCC should be performed in centration with the lens center [19]. In conventional cataract surgery, most surgeons prefer to use the PC as the center for CCC because of convenience and the difficulty of detecting the actual lens center.

Unlike lens-centered capsulotomy, pupil-centered capsulotomy does not provide 360° overlap of the optic edge. In one study that focused on optic edge overlap and IOL position, the lens-centered method offered better IOL positioning in 82% of eyes while 9% were in a better position after pupil-centered capsulotomy. In addition, 100% of the eyes that underwent lens-centered capsulotomy exhibited 360° optic overlap by the capsule compared to only 78% of eyes that underwent pupil-centered capsulotomies [22].

The presence of angle kappa in normal human eyes is due to the eye not being a centered optical system. Therefore, controversy remains over the correct centering location for laser refractive surgical treatment and MFIOL implantation. Temporal decentration of the IOL causes more problems when implanting a multifocal IOL. Especially with a high-angle kappa, the risk of postoperative photic phenomena is higher [9,23]. In corneal refractive surgery, a large angle kappa increases the risk for decentration of the optical zone from the VA if ablation is centered over the entrance pupil. Such decentration can cause many optical problems, induce astigmatism and prevent visual deficit correction, especially in hyperopic patients [11,24,25].

Both VA/angle kappa and the lens center can influence visual outcomes after cataract and corneal refractive surgery. However, those values are typically not available intraoperatively in the surgical field. The results of this study suggest that the PC was close to both the lens center and the VA, but the lens center was significantly closer. This knowledge of the positional relationships of various centers will be helpful, especially in the capsulotomy stage.

Based on the lens center, the LC was more inferior and temporal in location compared to the PC. This finding can be understood based on physiologic phenomena. In previous studies, the PC is located more nasally and superiorly than the LC in the dilated state, and mydriasis causes the PC to be displaced nasally and superiorly [26-28]. However, there was no significant location difference between the PC and LC based on the VA; however, this could have been affected by the small sample size of this study.

There are several limitations to this study. The location of the lens center cannot be measured based on the contour of the crystalline lens through the built-in Catalys system device. Since the 3D-OCT used in the Catalys system cannot completely evaluate retro-iris structures, the software extrapolates the anterior and posterior capsule lines of the crystalline lens to calculate the lens center. However, in a

study on postoperative IOL center location, the scanned capsule and angle centers were similar to each other. In addition, according to a lens center location study that examined ex-vivo porcine eyes using high-resolution magnetic resonance imaging, the angle center is the nearest marker to the center of the lens equator, which is similar to the location of the scanned capsule center [29].

The relatively small sample size of this study may have affected its statistical power. Therefore, the results should be interpreted with caution. We conducted a retrospective study, so additional research is necessary to compare clinical outcomes between various centers as CCC centers. Although we cross-checked the measurements, we used image conversion and a processing program (ImageJ). As a result, there could be minor errors affecting the accuracy of location measurement. Finally, poorly dilated pupils need to be evaluated in future studies.

In summary, this study demonstrated the positional and locational relationships between centers in cataract and refractive surgery. Surgeons should be aware of these positional relationships when performing conventional cataract surgery, especially in the capsulotomy stage.

Conflict of Interest

No potential conflict of interest relevant to this article was reported.

References

1. Gimbel HV, Neuhann T. Development, advantages, and methods of the continuous circular capsulorhexis technique. *J Cataract Refract Surg* 1990;16:31-7.
2. Gimbel HV, Neuhann T. Continuous curvilinear capsulorhexis. *J Cataract Refract Surg* 1991;17:110-1.
3. Mutlu FM, Bilge AH, Altinsoy HI, Yumusak E. The role of capsulotomy and intraocular lens type on tilt and decentration of polymethylmethacrylate and foldable acrylic lenses. *Ophthalmologica* 1998;212:359-63.
4. Taketani F, Matuura T, Yukawa E, Hara Y. Influence of intraocular lens tilt and decentration on wavefront aberrations. *J Cataract Refract Surg* 2004;30:2158-62.
5. Baumeister M, Buhren J, Kohnen T. Tilt and decentration of spherical and aspheric intraocular lenses: effect on higher-order aberrations. *J Cataract Refract Surg* 2009;35:1006-12.
6. Hayashi K, Hayashi H, Nakao F, Hayashi F. Anterior capsule contraction and intraocular lens decentration and tilt after hydrogel lens implantation. *Br J Ophthalmol* 2001;85:1294-7.
7. Moshirfar M, Hoggan RN, Muthappan V. Angle Kappa and its importance in refractive surgery. *Oman J Ophthalmol* 2013;6:151-8.
8. Prakash G, Prakash DR, Agarwal A, et al. Predictive factor and kappa angle analysis for visual satisfactions in patients with multifocal IOL implantation. *Eye (Lond)* 2011;25:1187-93.
9. Hayashi K, Hayashi H, Nakao F, Hayashi F. Correlation between pupillary size and intraocular lens decentration and visual acuity of a zonal-progressive multifocal lens and a monofocal lens. *Ophthalmology* 2001;108:2011-7.
10. de Vries NE, Webers CA, Touwslager WR, et al. Dissatisfaction after implantation of multifocal intraocular lenses. *J Cataract Refract Surg* 2011;37:859-65.
11. Soler V, Benito A, Soler P, et al. A randomized comparison of pupil-centered versus vertex-centered ablation in LASIK correction of hyperopia. *Am J Ophthalmol* 2011;152:591-9.
12. Kermani O, Oberheide U, Schmiedt K, et al. Outcomes of hyperopic LASIK with the NIDEK NAVEX platform centered on the visual axis or line of sight. *J Refract Surg* 2009;25:S98-103.
13. Packer M, Teuma EV, Glasser A, Bott S. Defining the ideal femtosecond laser capsulotomy. *Br J Ophthalmol* 2015;99:1137-42.
14. Cekic O, Batman C. The relationship between capsulorhexis size and anterior chamber depth relation. *Ophthalmic Surg Lasers* 1999;30:185-90.
15. Tackman RN, Kuri JV, Nichamin LD, Edwards K. Anterior capsulotomy with an ultrashort-pulse laser. *J Cataract Refract Surg* 2011;37:819-24.
16. Nagy ZZ, Kranitz K, Takacs AI, et al. Comparison of intraocular lens decentration parameters after femtosecond and manual capsulotomies. *J Refract Surg* 2011;27:564-9.
17. Friedman NJ, Palanker DV, Schuele G, et al. Femtosecond laser capsulotomy. *J Cataract Refract Surg* 2011;37:1189-98.
18. Kranitz K, Takacs A, Mihaltz K, et al. Femtosecond laser capsulotomy and manual continuous curvilinear capsulorrhexis parameters and their effects on intraocular lens centration. *J Refract Surg* 2011;27:558-63.
19. Park JH, Lee KH, Lee DJ. Comparison of continuous curvilinear capsulorhexis parameters between femtosecond laser and conventional cataract surgery. *J Korean Ophthalmol Soc* 2014;55:1800-7.

20. Mihaltz K, Knorz MC, Alio JL, et al. Internal aberrations and optical quality after femtosecond laser anterior capsulotomy in cataract surgery. *J Refract Surg* 2011;27:711-6.
21. Filkorn T, Kovacs I, Takacs A, et al. Comparison of IOL power calculation and refractive outcome after laser refractive cataract surgery with a femtosecond laser versus conventional phacoemulsification. *J Refract Surg* 2012;28:540-4.
22. Bafna, S. *Capsulotomy centration in laser cataract surgery*. [place unknown]: Eyeworld Asia-Pacific; 2014. p. 33-4.
23. Rosales P, De Castro A, Jimenez-Alfaro I, Marcos S. Intraocular lens alignment from purkinje and Scheimpflug imaging. *Clin Exp Optom* 2010;93:400-8.
24. Basmak H, Sahin A, Yildirim N, et al. Measurement of angle kappa with synoptophore and Orbscan II in a normal population. *J Refract Surg* 2007;23:456-60.
25. Kanellopoulos AJ. Topography-guided hyperopic and hyperopic astigmatism femtosecond laser-assisted LASIK: long-term experience with the 400 Hz eye-Q excimer platform. *Clin Ophthalmol* 2012;6:895-901.
26. Yang Y, Thompson K, Burns SA. Pupil location under mesopic, photopic, and pharmacologically dilated conditions. *Invest Ophthalmol Vis Sci* 2002;43:2508-12.
27. Walsh G. The effect of mydriasis on the pupillary centration of the human eye. *Ophthalmic Physiol Opt* 1988;8:178-82.
28. Wyatt HJ. The form of the human pupil. *Vision Res* 1995;35:2021-36.
29. Lee YE, Joo CK. Assessment of lens center using optical coherence tomography, magnetic resonance imaging, and photographs of the anterior segment of the eye. *Invest Ophthalmol Vis Sci* 2015;56:5512-8.